

A Five-Degree-of-Freedom Hybrid Manipulator for Machining of Complex Curved Surface

Yundou Xu^{1,2}, Jianhua Hu¹, Dongsheng Zhang¹, Jiantao Yao^{1,2},
and Yongsheng Zhao^{1,2(✉)}

¹ Parallel Robot and Mechatronic System Laboratory of Hebei Province,
Yanshan University, Qinhuangdao 066004, China
yszhao@ysu.edu.cn

² Key Laboratory of Advanced Forging & Stamping Technology and Science
of Ministry of National Education, Yanshan University,
Qinhuangdao 066004, China

Abstract. In this paper, a novel five-axis hybrid manipulator is constructed based on the 2-RPU&UPR parallel mechanism, which has less joints and all the axes of rotation are continuous. Then, the structure of the key components of the new five-axis hybrid manipulator is designed. Next, the analytic expression of the inverse position of the hybrid manipulator is established, based on which, the workpiece of the spherical surface is machined. All rotational degrees of freedom of this five-axis hybrid manipulator are of continuous axes, the analytical expression of the inverse position model can be obtained, so the trajectory planning and motion control can be realized easily. Moreover, the hybrid manipulator has less joints, which can guarantee high rigidity and high precision operation, so it has great application prospects.

Keywords: Hybrid manipulator · Parallel mechanism · Continuous axes · Inverse position

1 Introduction

In the high-precision machining of aerospace structural parts with large size, thin-walled and complex surfaces, the five-degree-of-freedom (DOF) serial-parallel hybrid robots have become more and more concerned by academia and industry [1, 2]. That is because the hybrid robot, as the compromise between parallel robots and series robots, has the characteristics of high rigidity, large workspace and high flexibility simultaneously [3, 4]. The five-DOF hybrid robots [5, 6] such as Tricept and Sprint Z3 head have been successfully applied in the field of aerospace processing, as well as automotive and aviation assembly, welding, drilling and so on.

The existing five-DOF hybrid robots can be classified into two categories [7]. The first category is composed of a three-DOF position parallel mechanism (3-UPS&UP [8], 2-UPS&UP [9], 2-UPR&SPR [10] parallel mechanism for example) plusing a 2-DOF rotating head attached to the moving platform, which has been exemplified successfully by Tricept hybrid robot. Here, U, P, S and R denote the universal,

prismatic, spherical and rotational joints, respectively. The second category is the integration of a three-DOF pose parallel mechanism (3-PRS [11], 3-RPS [12] parallel mechanism for example) and two long guideways, which has been exemplified successfully by Sprint Z3 Head hybrid robot. However, these three-DOF parallel mechanisms above have a large number of joints, restricting the overall stiffness of the hybrid robot and operating accuracy. Based on a three-DOF parallel mechanism 2-RPU&UPR with less joints (the number of passive single-DOF joints is only 9 except the driven joints), a new five-DOF hybrid robot is constructed in this paper, which has the advantages of less joints, so it can meet the needs of high rigidity and high precision, and the application prospects is broad.

2 The Structure Composition of the Five-DOF Hybrid Manipulator

2.1 Principle Analysis of the Five-DOF Hybrid Robot Mechanism

As shown in Fig. 1, the robot consists of 2-RPU&UPR parallel mechanism, a head with one revolute joint, a mobile platform and the frame. The mechanism diagram is shown in Fig. 2. The 2-RPU&UPR mechanism has two rotational and one translational degrees of freedom, which are the rotation around the Y -axis on the fixed platform, the rotation of the x -axis on moving platform and the translation around of the Z -axis on the fixed platform. The rotation around the x -axis is used for the attitude adjustment in x -axis, while the rotation around the Y -axis are used to adjust a wide range of movement along X -axis. Therefore, a head with a revolute joint whose axis is parallel to the Y -axis, is connected to moving platform under the parallel mechanism to achieve attitude adjustment in y -direction, and a separate mobile platform along the Y -axis is installed on the workbench, so as to achieve the five-axis motions simultaneously.

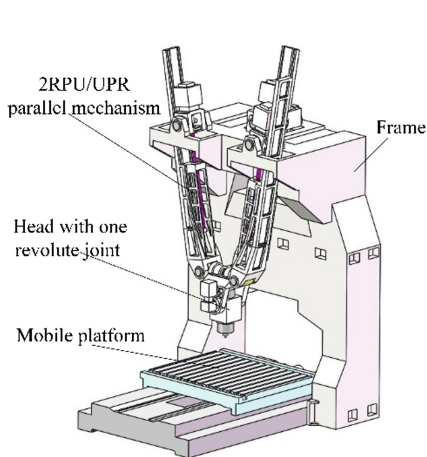


Fig. 1. Overall structure of 5-DOF hybrid robot

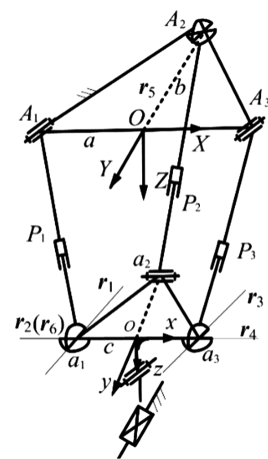


Fig. 2. Diagram of 5-DOF hybrid robot

2.2 Structural Design Principle

The Moving Platform

Three actuated branches and the head with one revolute joint are all connected to the moving platform, so two Hooke joints and two joints need to be designed on this moving platform, the structure model of the moving platform is designed as shown in Fig. 3.

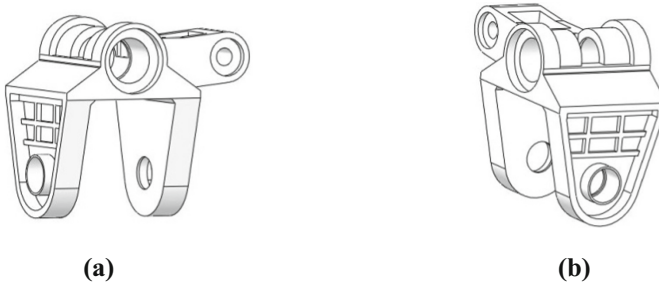


Fig. 3. Structure model of moving platform

In order to make the structure compact and reduce the distance between the motorized spindle and the moving platform, the driving motor of the head with one revolute joint is arranged at the front end of the moving platform. The relationship between the moving platform and the motorized spindle is shown in Fig. 4.

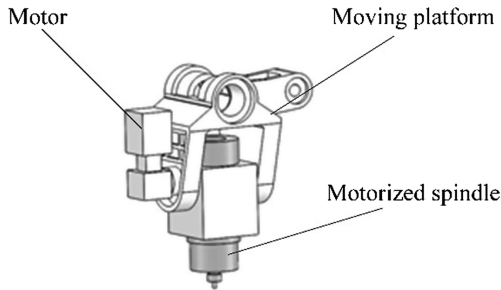


Fig. 4. Assembly diagram of the moving platform and the motorized spindle

Branches 1 and 2 are respectively connected to the moving platform by universal joints, branch 3 is connected to the moving platform through a revolute joint, as shown in Fig. 5. Since branches 1 and 2 are symmetrically arranged with respect to the moving platform, the two U joints are designed as T-shaped structures. Long end of two T heads are arranged coaxially. The two short heads on the other side of the T-shaped structures connect the branches in the same way, as shown in Fig. 6. Branch 3 is connected to the moving platform as shown in Fig. 7.

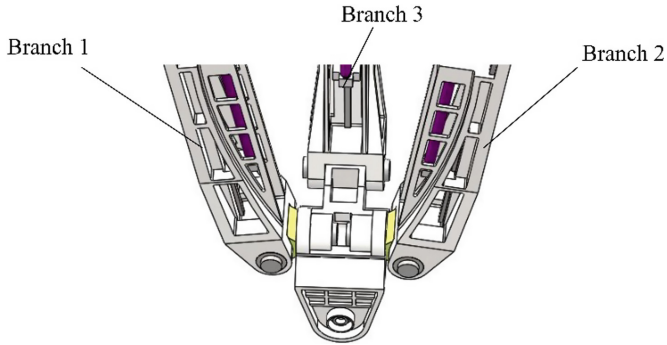


Fig. 5. Structure of connection for branches and moving platform

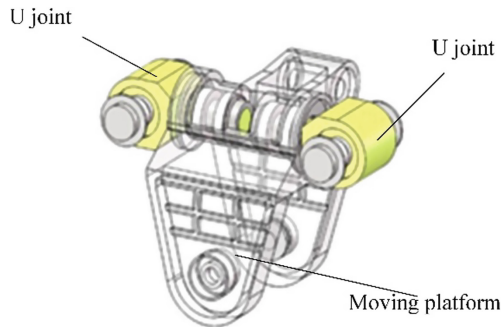


Fig. 6. Moving platform and U joints

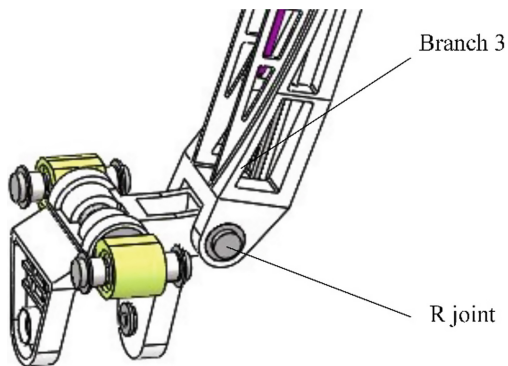


Fig. 7. Revolute joint and branch 3

The Design of Branches

The structure of the branches plays an important role in the performance of the whole hybrid manipulator, and its structure is divided into two types: fixed length and variable

length. The fixed length is better than the variable length in rigidity and is easy to be manufactured.

In this paper, the design of three branches of the hybrid manipulator all adopts the form of fixed length. In order to make the structure more compact and reduce the quality, select the DC servo motor with smaller diameter to drive the ball screw rotating. The ball screw is supported by both ends to increase the rigidity and motion stability of the linear drive unit, one end is connected with the screw nut which is fixed at the upper end of the branch rod, and the other end is connected with the screw support base. The specific structure of the branch is shown in Fig. 8.

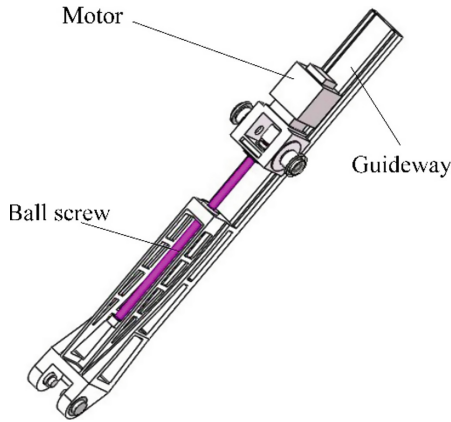


Fig. 8. Structure of branches

Branches 1 and 2 are connected to the fixed platform by means of revolute joints. The servo motor is arranged directly on the upper end of the R joint. The R joint is fixed on the frame and can only rotate relative to the frame, as shown in Fig. 9. The branch 3 is connected to the fixed platform by means of a U joint, the specific structure is shown in Fig. 10.

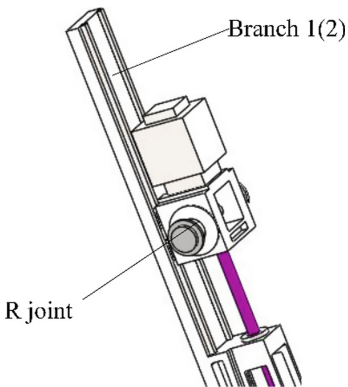


Fig. 9. Structure of R joint

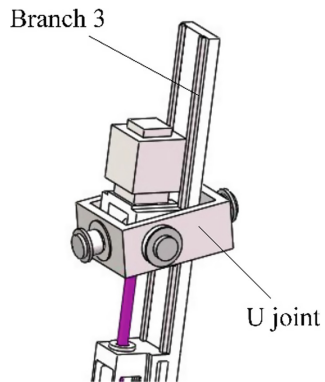


Fig. 10. Structure of U joint

2.3 Design of the Frame

The frame of the hybrid manipulator is a component which is connected with the worktable and the ground, whose stiffness and strength directly affect the accuracy and life of the manipulator. In this paper, the fixed platform is integrated with the frame, the overall structure uses welding parts. The specific structure of the frame is shown in Fig. 11.

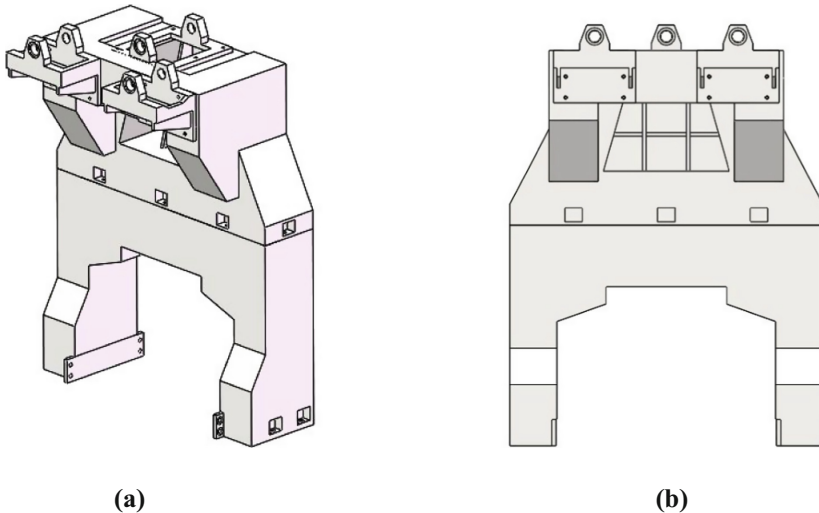


Fig. 11. Structure of the frame

3 Realization of Complex Surface Machining

3.1 Solution of Inverse Position

It can be seen from the literature [13] that the 2-RPU&UPR parallel mechanism has a translation and two rotations with continuous axes, so that the moving platform can obtain the pose through the following three transformations. Firstly rotates θ_1 around the Y -axis; then translate λ along the Z -axis; finally rotates θ_2 around the x -axis, so the mechanism can be equivalent to a serial mechanism composed of three joints of R, P and R. Consequently, the entire hybrid robot can be equivalent to a combination of a RPRR serial mechanism and a moving platform, as shown in Fig. 12, so the solving of the inverse position of the hybrid robot can be greatly simplified.

Next, we establish inverse position model of the hybrid robot. Since the hybrid robot consists of the 4-DOF serial mechanism RPRR and the 1-DOF mobile platform equivalently (the moving direction is along the y_0 -direction), the orientation and the displacement in the x_0 -axis and z_0 -axis required for machining the workpiece are directly determined by the serial mechanism RPRR. While the displacement in the

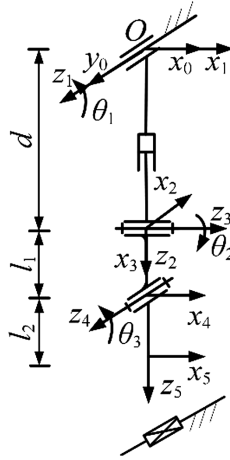


Fig. 12. Equivalent mechanism of the hybrid robot

y_0 -direction needs to be determined by the tool and mobile platform, since the serial mechanism generates a part of coupling displacement in y -axis.

Define the following parameters:

- θ_1 — The angle of the first R joint of the equivalent serial mechanism RPRR;
- θ_2 — The angle of the second R joint of the equivalent serial mechanism RPRR;
- θ_3 — The angle of the third R joint of the equivalent serial mechanism RPRR;
- d_0 — The distance between the fixed platform and the moving platform in the initial state;
- d_1 — The displacement of the P joint of the equivalent serial mechanism RPRR;
- d_2 — The displacement of mobile platform in the y_0 -direction;
- $[a_x \ a_y \ a_z]^T$ — The direction of the tool;
- $[p_x \ p_y \ p_z]^T$ — The position of the end of the tool;
- y_0 — The displacement of workpiece in the y_0 -direction.

According to the D-H method, the analytical expression of the inverse position solution can be obtained as follows:

$$\begin{cases} \theta_1 = \arctan[(-a_x l_2 + p_x)/(-a_z l_2 + p_z)] \\ \theta_3 = \arcsin(a_x c_1 - a_z s_1) \\ \theta_2 = \arcsin(-a_y/c_3) \\ d_1 = (-a_z l_2 + p_z - l_1 c_1 c_2)/c_1 - d_0 \\ d_2 = -a_y l_2 + a_y l_1/c_3 - y_0 \end{cases} \quad (1)$$

3.2 Examples: Spherical Surface Machining

As shown in Fig. 13, assuming that the locus of the workpiece to be machined is a sphere, the spherical radius is R , The radius of the circular trajectory being processed of the tool is r , so the distance between the center of the workpiece and the center of the circle being processed is $m = \sqrt{R^2 - r^2}$, and the distance between the center of the circle being processed and the $\{0\}$ coordinate system of the machine is h . the angle between the x -axis and the straight line connecting the center of the circle and the processing point is α .

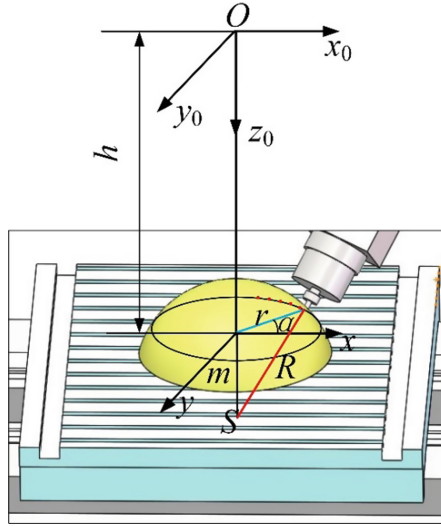


Fig. 13. Machining trajectory of workpiece

The position of the current processing point is:

$$(r \cos \alpha \quad -r \sin \alpha \quad h)^T, \alpha \in (0, 360^\circ)$$

Here requires the normal of the tool and the tangent plane of the processing point are vertical, so the direction of the tool should be:

$$(-r \cos \alpha / R \quad r \sin \alpha / R \quad m / R)^T$$

That is:

$$(a_x \quad a_y \quad a_z) = (-r \cos \alpha / R \quad r \sin \alpha / R \quad m / R) \quad (2)$$

Since the workpiece moves only in the y -direction of the $\{0\}$ system on the mobile platform, the x and z coordinates of the tool and the workpiece in the $\{0\}$ system are the

same at any time, then the x and z coordinates of the origin of $\{5\}$ system in the $\{0\}$ system are:

$$\begin{cases} p_x = r \cos \alpha \\ p_z = h \end{cases} \quad (3)$$

Substituting (2) and (3) into (1) yields:

$$\begin{cases} \theta_1 = \arctan[r(R + l_2)c\alpha / (Rh - ml_2)] \\ \theta_3 = \arcsin\left[\left(-rc\alpha c_1 - s_1\sqrt{R^2 - r^2}\right) / R\right] \\ \theta_2 = \arcsin[-rs\alpha / (Rc_3)] \\ d_1 = (Rh - ml_2 - Rl_1c_1c_2) / (Rc_1) - d_0 \\ d_2 = (-rs\alpha c_3l_2 - rs\alpha l_1 + Rrs\alpha c_3) / (Rc_3) \end{cases} \quad (4)$$

3.3 Simulation

Given a specific set of parameters for the structure of the robot and the machining path of the workpiece, as follows: $a = 400$ mm, $b = 300$ mm, $c = 200$ mm, $r_{10} = 824.62$ mm, $r_{20} = 813.94$ mm, $r_{30} = 824.62$ mm, $l_1 = 50$ mm, $l_2 = 60$ mm, $r = 60$ mm, $R = 100$ mm, $m = 80$ mm, $h = 150$ mm. Then d_0 can be calculated according to the structural parameters of the robot for 800 mm, substituting the given parameters into (4), the following results can be obtained:

$$\begin{cases} \theta_1 = \arctan(16c\alpha / 17) \\ \theta_3 = \arcsin(-0.6c\alpha c_1 - 0.8s_1) \\ \theta_2 = \arcsin(-0.6s\alpha / c_3) \\ d_1 = (102 - 50c_1c_2) / c_1 - d_0 \\ d_2 = (36s\alpha c_3 - 30s\alpha - y_0c_3) / c_3 \end{cases}$$

For the (2-RPU&UPR) + R four-DOF mechanism, substitute the result of the inverse solution into the positive solution, we can get the direction and position of the tool's end. Figure 14 shows the track of the tool's direction. It can be seen from the figure that the orientation is exactly the same as that of the tool in processing the workpiece. The position of the workpiece is determined by that of the (2-RPU&UPR) + R four-DOF mechanism and the 1-DOF mobile platform, and the resulting position trajectory of workpiece is shown in Fig. 15. It can be seen from the figure that the track of the workpiece is a circle and its radius is 60, which is exactly the same as the pre-machined track of workpiece given earlier.

The previous analyses show that the hybrid robot can realize the linkage processing of the complex surface of the workpiece, and also verify that the inverse position model of the hybrid robot is completely correct.

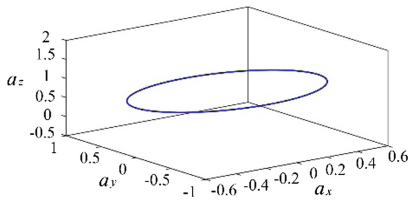


Fig. 14. Track of tool's orientation

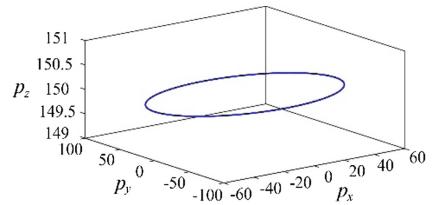


Fig. 15. Position of workpiece

4 Conclusion

A five-DOF hybrid manipulator is constructed based on the two-rotation-and-one-translation three-DOF parallel mechanism of 2-RPU&UPR. All the rotational axes of the robot are continuous and the robot has less number of passive joints. The key components are designed with reasonable structure, ensuring its high structural rigidity characteristics, so it can meet the needs of high precision operation.

The analytical expression of the position model of the robot is obtained, and the model is validated through the machining of a workpiece with spherical surface. The simulation results show that the robot can continuously adjust the attitude, so as to keep the normal of the tool and the normal of the machining surface coincident, and can finally finish the machining of the spherical surfaced workpiece.

Acknowledgment. This work was supported by the National Natural Science Foundation of China under Grant 51405425, and Key Basic Research Program of Hebei Province's Applied Basic Research Plan of China under Grant 15961805D.

References

1. Liu, N., Wu, J.: Kinematics and application of a hybrid industrial robot-Delta-RST. *Sens. Transducers* **169**, 186–192 (2014)
2. Terrier, M., Dugas, A., Hascoët, J.Y.: Qualification of parallel kinematics machines in high-speed milling on free form surfaces. *Int. J. Mach. Tools Manuf.* **44**(7–8), 865–877 (2004)
3. Hunt, K.H.: Structural kinematics of in-parallel-actuated robot-arms. *J. Mech. Transmissions Autom. Des.* **105**(4), 705–712 (1983)
4. Xie, F.G., Liu, X.J., Zhang, H., et al.: Design and experimental study of the SPKM165, a five-axis serial-parallel kinematic milling machine. *Sci. China Technol. Sci.* **54**(5), 1193–1205 (2011)
5. Wang, Y.Y., Huang, T., Zhao X.M., et al.: Finite element analysis and comparison of two hybrid robots-the tricept and the trivariant. In: *IEEE/RSJ International Conference on Intelligent Robots and Systems*, pp. 490–495 (2006)
6. Shi, J., Wang, Y., Zhang, G., et al.: Optimal design of 3-DOF PKM module for friction stir welding. *Int. J. Adv. Manuf. Technol.* **66**(9–12), 1879–1889 (2013)

7. Lian, B., Sun, T., Song, Y., et al.: Stiffness analysis and experiment of a novel 5-DoF parallel kinematic machine considering gravitational effects. *Int. J. Mach. Tools Manuf.* **95**, 82–96 (2015)
8. Siciliano, B.: The Tricept robot: inverse kinematics, manipulability analysis and closed-loop direct kinematics algorithm. *Robotica* **17**, 437–445 (1999)
9. Sun, T., Song, Y.M., Li, Y.G., Zhang, J.: Workspace decomposition based dimensional synthesis of a novel hybrid reconfigurable robot. *J. Mech. Robot.* **2**(3), 031009-1–031009-8 (2010)
10. Bi, Z.M., Jin, Y.: Kinematic modeling of Exechon parallel kinematic machine. *Robot. Comput.-Integr. Manuf.* **27**(1), 186–193 (2011)
11. Sun, T., Song, Y.M.: Dimensional synthesis of a 3-DOF parallel manipulator based on dimensionally homogeneous Jacobian matrix. *Sci. China Technol. Sci.* **53**(1), 168–174 (2010)
12. Schadlbauer, J., Walter, D.R., Husty, M.L.: The 3-RPS parallel manipulator from an algebraic viewpoint. *Mech. Mach. Theory* **75**(5), 161–176 (2014)
13. Xu, Y., Zhou, S., Yao, J., et al.: *Rotational Axes Analysis of the 2-RPU/SPR 2R1T Parallel Mechanism*, 2nd edn. Springer, Cham (2014)